ISBN: 978-3-95450-232-5 ISSN: 2673-7000 doi:10.18429/JACoW-NAPAC2022-THZD1

INSTANT PHASE SETTING IN A LARGE SUPERCONDUCTING LINAC *

A. S. Plastun, P. N. Ostroumov
Facility for Rare Isotope Beams (FRIB), Michigan State University, East Lansing, MI, USA

Abstract

The instant phase setting reduces the time needed to setup 328 radiofrequency cavities of the Facility for Rare Isotope Beams (FRIB) linac from 20 hours to 10 minutes. This technique uses a 1-D computer model of the linac to predict the cavities' phases. The model has been accurately calibrated using the data of the 360-degree phase scans — a common procedure for phasing of linear accelerators. The model was validated by comparison with a conventional phase scan results. The predictions applied to the linac are then verified by multiple time-of-flight energy measurements and the response of the beam position/phase monitors (BPMs) to an intentional energy and phase mismatch.

The presented approach not just reduces the time and the effort required to tune the FRIB accelerator for new experiments every couple of weeks, but it also provides an easy recovery from cavity failures. It is beneficial for user facilities requiring high beam availability, as well as for radioactive ion beam accelerators, where quick time-of-flight energy measurement via the BPMs is not possible due to the low intensities of these beams.

INTRODUCTION

The Facility for Rare Isotope Beams (FRIB) is a new U.S. Department of Energy (DOE) Office of Science user facility [1]. Maintaining high beam variability and availability are our goals. The variability is important because the user experiments last only about a week or two, and the facility needs to be quickly retuned for a new user. The beam availability is essential for good user experience and scheduling of the experiments.

The FRIB driver linac is a folded superconducting RF (SRF) accelerator, as shown in Fig. 1. The number of independently phased RF cavities in the linac is 328 [2–4] (see Table 1), which makes it very flexible for acceleration of various ion species to different energies. Changing the beam velocity profile requires the rephasing of many cavities. The variance of the energy loss of different ion species in the charge stripper makes scaling from one beam to another challenging. When the tune is established and the experiment is running, statistically the chance of a cavity (or its RF circuit) failure is not negligible [5]. The fault scenarios may require the retuning of several cryomodules or even linac segments. If it is done by conventional phase scans, it takes many hours. In this paper, we describe a model-based phasing approach that allows us to change velocity profiles in just several minutes.

* This work is supported by the U.S. Department of Energy Office of Science under Cooperative Agreement No. DE-SC0000661, the State of Michigan, and Michigan State University.

PHASING OF A LINEAR ACCELERATOR

Tuning of field amplitudes and phases of cavities is intended to match the design velocity profile and to provide sufficient stability of longitudinal motion of the beam particles [6]. Usually, it is performed by a phase scan procedure when the cavity phase is scanned in a range of up to 360° and the beam energy is measured. The measurement can be done in different ways, for example, using a sole calibrated dipole magnet [7] or in a combination with a beam position detector [11], using silicon detectors [8, 9], or various time-of-flight techniques by means of gamma-ray detectors [7], fast current transformers [10], beam position/phase monitors (BPPMs or BPMs) [12, 13] and even cavities as the beam phase detectors [14, 15]. The measurements are usually fitted into a model, which sets cavities to a given accelerating (also known as synchronous or reference) phase.

A first-order model, coupling the input W_{in} and output W_{out} beam energies, follows from the Panofsky equation [6, 16] (which was originally derived for an accelerating gap of a drift-tube linac) and can be written as:

$$W_{\text{out}} = W_{\text{in}} + \Delta W_{\text{max}} \cos(\varphi_{\text{cav}} + \Delta\varphi), \quad (1)$$

here ΔW_{max} is the maximum energy gain of a charged particle, which can be achieved in the cavity at a given field level, φ_{cav} is the cavity phase control variable, and $\Delta\varphi$ is the phase offset of the cosine-like waveform which depends on delays in the cavity's RF circuits and the beam arrival time to the cavity. The cavity is tuned to a given synchronous phase φ_s when $\varphi_{\text{cav}} + \Delta\varphi = \varphi_s$. Assuming the input energy is known from the phasing of an upstream cavity, Eq. (1) has two unknowns, namely the ΔW_{max} and the $\Delta\varphi$, which can be found from at least two sets of (φ_{cav},W_{out}).

In SRF linacs phase scans may look significantly different from a cosine curve due to high accelerating field amplitudes and low beam energies. Figure 2 presents several examples obtained by particle tracking, as well as their first and second-order approximations [17]. In such cases, the cavity phase φ_{cav} corresponding to the desired φ_s should be set in the same way as the particle tracking (beam dynamics) codes do that.

Table 1: FRIB Linac Cavities

Type	#	Segments	β_{opt}	V_a (MV)
Buncher	2	MEBT	0.038	0.10
QWR041	12	LS1	0.043	0.81
QWR085	92	LS1, FS1	0.086	1.78
IH-Buncher	2	FS1	0.185	1.00
HWR029	72	LS2	0.290	2.09
HWR053	148	LS2, FS2, LS3	0.543	3.70

ISBN: 978-3-95450-232-5 ISSN: 2673-7000 doi:10.18429/JACoW-NAPAC2022-THZD1

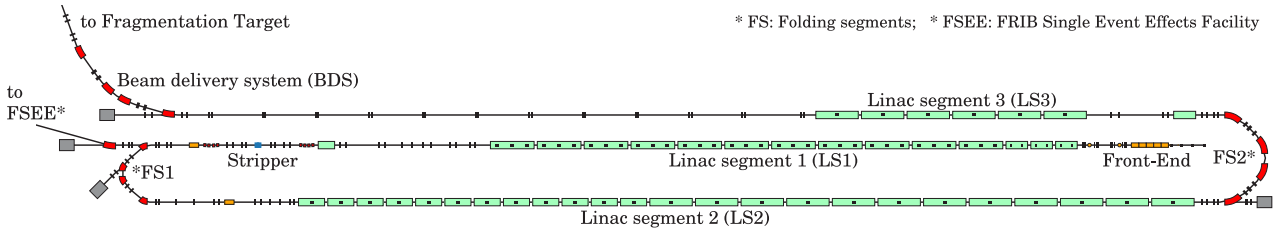

Figure 1: Layout of the FRIB driver linac.

At FRIB, for example, we use the TRACK code [20] for beam dynamics simulations. TRACK sets φ_{cav} by getting the phase of the maximum energy gain, and adding the φ_s to it. In order to find the maximum energy gain phase, TRACK does several steps. First, it calculates the energy gain of a reference particle for 900 values of φ_{cav} uniformly distributed in the range of $[-180°, 180°]$. Then the code creates a cubic spline using these data and evaluates it at 36,000 points in the same 360°-range. Finally, it selects the point giving the highest energy, which is then added to φ_s and set as φ_{cav}. This procedure is performed sequentially for every cavity in the lattice.

History of Phase Scans at FRIB

Beam commissioning of the FRIB SRF linac started in July 2018. Twelve QWR041 cavities (see Table 1) accelerated the $^{40}Ar^{9+}$ beam to 2 MeV/u. A simple one-page-long python script scanned φ_{cav} with 10° steps and measured the phase signal of the nearest downstream BPM. Following the TRACK phase setting procedure, the measured data were interpolated by a cubic spline and displayed to the user. The phase corresponding to the minimum of the curve (i.e. the maximum energy gain) was found by eye, added to the given φ_s, and set as the cavity operating phase. The accuracy of the setpoint obviously could not exceed 5°. The field setpoints in the cavities were set based on rf field calibration and were not adjusted to match the simulated velocity profile. Tuning of these twelve cavities took about 5 hours.

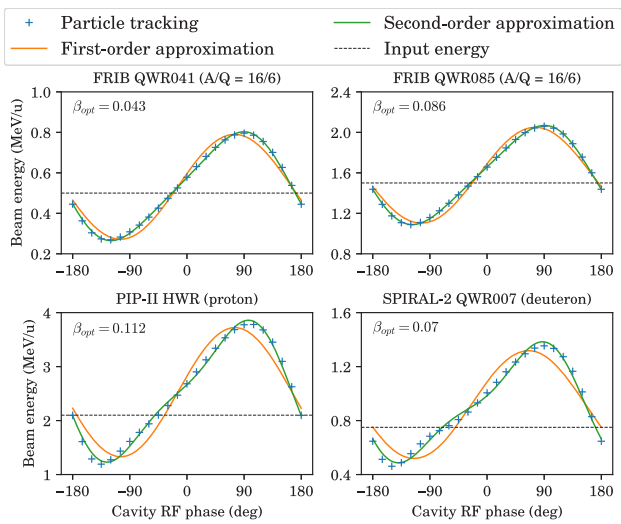

Figure 2: Phase scans of SRF cavities and their approximations. The field levels are at the design values. The field maps of the PIP-II [18] and SPIRAL2 [19] cavities used for these calculations are not exact.

The next commissioning stage was completed in February 2019 and made the FRIB driver accelerator the highest energy continuous-wave hadron linac in the world. The acceleration was done in an LS1 segment of the linac, which includes 14 cryomodules housing 100 SRF cavities. The need for automated phase scans was clear after the previous commissioning run. An extrapolation from 12 cavities in 5 hours to 100 cavities gives 42 hours or five 8-hour shifts.

We developed a high-level application (HLA) to automate most of the cavity tuning work. The turn-on procedure for LS1 cavities was already automated by that time [21, 22]. The HLA turned on cavities, performed phase scans, set requested synchronous phases, saved the scan data, and it could do that for a sequence of cavities with no human intervention. The HLA was called ALPha, which states for an Automated Linac Phasing.

ALPha used a difference of two BPMs' phase signals to find the cavity's phase of maximum energy gain. It did 30° steps, measured the BPM phases at every step, built a cubic spline with these data, evaluated it at 0.05° steps, and selected the point with the lowest BPM phase difference. And as before, this cavity phase was added to the synchronous phase value and set as an operating phase.

A new remarkable feature was that ALPha adjusted the field setpoints to match the simulated beam energies. The $^{40}Ar^{9+}$ beam reached the energy of 20.3 MeV/u in a total phasing time of about 10 hours, which also included the interleaved transverse trajectory corrections (which themselves were done manually at that time). Next two years we worked on minimizing the cavity turn-on time, increasing the field and phase ramp rates, using 5 Hz BPM data instead of 1 Hz, and reducing the number of the phase scan steps. Currently, phase setting for the whole LS1 still takes about 5 hours.

The beam commissioning of LS2 took place in March 2020, when 148 out of 168 SRF half-wave resonant cavities accelerated the fully-stripped $^{36}Ar^{18+}$ beam to 204.4 MeV/u in 12 hours. The automated turn-on was not available for LS2 cavities yet. When doing phase scans at the end of LS2, we had an issue related to their accuracy. First, the BPM signal strengths were lower than we observed at the beginning of LS2 because the voltage measured on the outputs

ISBN: 978-3-95450-232-5 ISSN: 2673-7000 doi:10.18429/JACoW-NAPAC2022-THZD1

of a button-like BPM is inversely proportional to the beam velocity [24]. Second, the beam energy was significantly higher than the energy gain in a single cavity. Therefore, the relative variation of the beam velocity and its time of flight during the phase scan was small. Third, the beam did not have a long drift space at the end of LS2 to accumulate any significant time of flight. A combination of these factors made the phase scan data noisier than we observed before. Reduction of the step size and taking more data samples at each step would help to overcome this problem. However, at that moment ALPha could make only one measurement per step and still used the cubic spline interpolation which in presence of measurement errors is prone to detect the point of maximum energy gain incorrectly. The next day after the beam commissioning, the code of ALPha was changed to fit a two-harmonic waveform [17] into the measured data. A comparison between interpolation and approximation of the measured phase scan data is presented in Fig. 3.

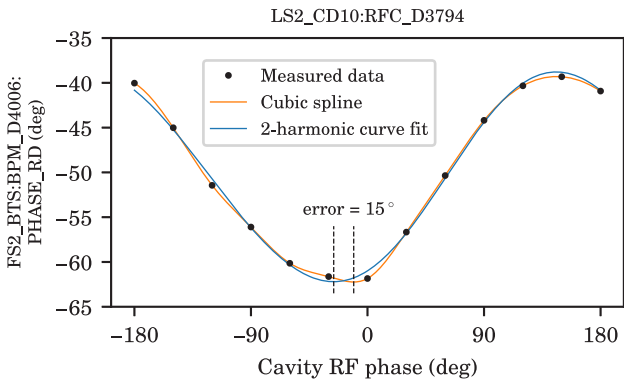

Figure 3: Cubic spline interpolation and 2-harmonic curve-fit approximation of the phase scan data.

Phase scans of the LS3 cavities do not have the accuracy problem thanks to a long drift section (see Fig. 1). Table 2 presents our best estimate of the time required for phase scans if they are done today. If one includes the time for trajectory correction, tuning of the folding segments, measurement of the charge state distribution after the charge stripper, and other necessary procedures, the tuning would take about 24 hours. When user experiments last only about a week or two, the tuning time significantly impacts the availability of the facility. The instant phase setting is, therefore, very demanded at FRIB.

Table 2: Phase Scan Duration

Segment	Cavities	Duration (HH:MM)
MEBT	2	0:10
LS1	12 + 88	5:00
FS1	4 + 2	0:20
LS2	168	12:00
FS2	4	0:15
LS3	48	2:00
Total	328	19:45

INSTANT PHASE SETTING

The instant phase setting (IPS) is a model-based tuning approach. The IPS model does not rely on any transit-time factor models and performs numerical integration of 1-D particle motion. The system of ordinary differential equations describing the phase trajectory of a particle can be written as

$$\begin{cases} \dfrac{dW}{dz} = qE_z(z,t), \\ \dfrac{dt}{dz} = \dfrac{1}{v_z}. \end{cases} \tag{2}$$

Here W is the particle kinetic energy, q is the charge of the particle, $E_z(z,t)$ is the longitudinal component of the electric field in the linac at the longitudinal position z and time t, v_z is the longitudinal component of the particle velocity and is related to the particle kinetic energy via formulas of relativistic mechanics [6]. Let us first consider a single-cavity case. The field distribution $E_z(z)$ in a cavity is simulated in CST Studio Suite [25], scaled by a coefficient K and the field setpoint A, and multiplied by a time term including the phase setpoint φ_{cav} of the cavity as follows:

$$E_z(z,t) = K \cdot A \cdot E_z(z) \cdot \cos(\omega t + \Delta\varphi + \varphi_{\text{cav}}). \tag{3}$$

Here $\Delta\varphi$ is a value representing a sum of all RF circuit delays and may be considered a phase offset of the cavity relative to the stable RF reference line, see Fig. 4. Every cavity and BPM have their own phase offsets. We assume they, as well as the K values, do not change unless the RF circuit has been changed. By solving Eq. (2) with initial conditions

$$\begin{cases} W(-L_{\text{cav}}/2) = W_0, \\ t(-L_{\text{cav}}/2) = t_0, \end{cases} \tag{4}$$

We get the beam energy at the exit of the cavity and the arrival time to this point. A set of parameters $(K, \Delta\varphi)$ is found by fitting the Eq. (2) solution to the measured phase

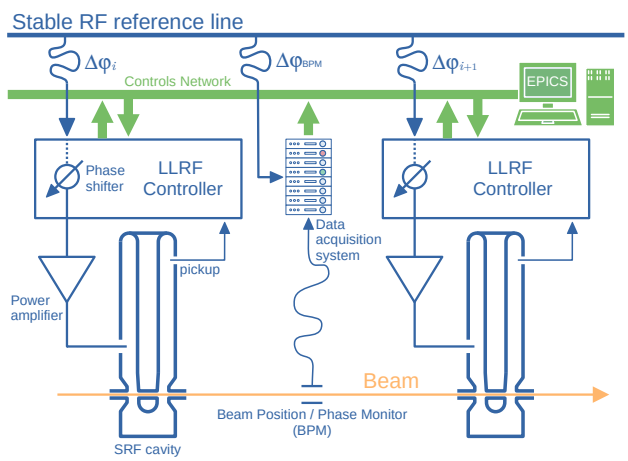

Figure 4: Simplified scheme of an RF system for a short segment of a linear accelerator.

ISBN: 978-3-95450-232-5 ISSN: 2673-7000 doi:10.18429/JACoW-NAPAC2022-THZD1

scan. In this text, we call it *cavity calibration*. A model-based tuning method developed at Spallation Neutron Source (SNS) [23] also uses similar techniques to fit the model parameters.

If a cavity is placed at $z = z_{\mathrm{cav}}$, Eq. (3) changes to

$$E_z(z,t) = K \cdot A \cdot E_z(z - z_{\mathrm{cav}}) \cdot \cos(\omega t + \Delta\varphi + \varphi_{\mathrm{cav}}). \quad (5)$$

Now, any sequence of N cavities can be described by a linear combination of Eq. (5) for every cavity:

$$E_z(z,t) = \sum_{n=1}^{N} K_n \cdot A_n \cdot E_z(z - z_n) \cdot \cos(\omega t + \Delta\varphi_n + \varphi_n). \quad (6)$$

The phase offsets of the model's BPMs can be calibrated in the same way as the cavities. The IPS models for each linear segment of the FRIB linac have been developed and calibrated using the previously obtained phase scan data. Accurate positions of cavities and BPMs are important for the calibration. We got them from the alignment survey data.

Validation

The first test of the IPS model was performed with the last 17 cavities of LS3. The synchronous phases of these cavities were varied from -10° to -90° with 10-deg steps, and the LS3 output energy was measured and compared with a cosine law. The plot of the data is shown in Fig. 5. A little discrepancy at -20° and -10° is due to the transit-time factor decrease in the cavities. That was a successful demonstration of the model-based phasing in the FRIB linac.

The next test was done with 72 HWR029 cavities in LS2 in the beginning of the liquid-lithium stripper commissioning. The cavities were phased by the IPS model, and then we turned off them sequentially to measure the output energies. Figure 6 presents the difference between the model prediction and the measurements. Despite the variation of the input LS2 energy, the energy difference is not accumulated toward the end of the HWR029 section.

A comparison between the phase scans performed by ALPha and the IPS model prediction was also done for

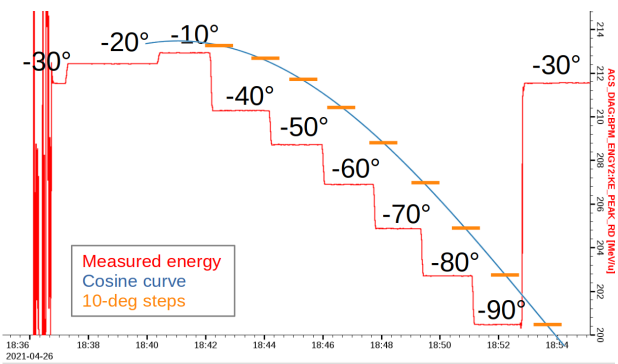

Figure 5: Model-based rephasing of last 17 LS3 cavities. Values on top of every step are the cavities' synchronous phases.

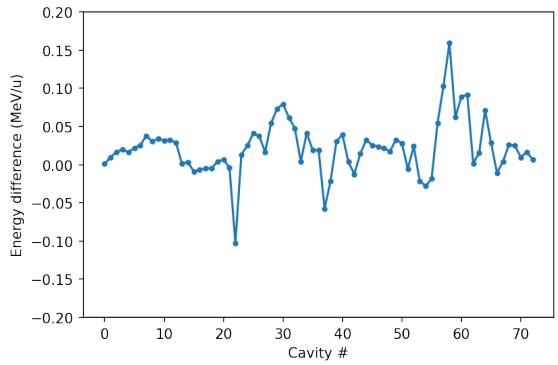

Figure 6: Difference between the measured and predicted beam energy after each of 72 HWR029 cavities in LS2.

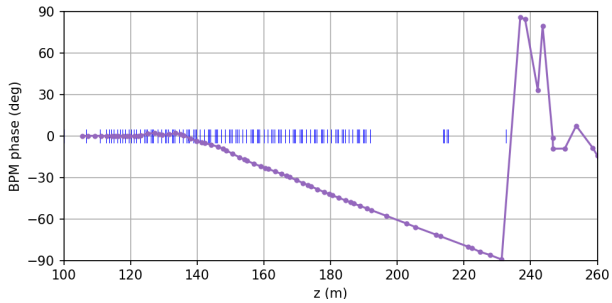

Figure 7: BPM phase difference between the LS1 velocity profile established by conventional phase scans and the one predicted by the IPS model.

88 LS1 QWR085 cavities. LS1 had been phased by ALPha to 17 MeV/u, and the phase scan data had been supplied to the IPS model and used to calibrate it. Then both ALPha and the IPS model phased LS1 to the same 20 MeV/u velocity profile, and we reviewed the difference in the BPM phases obtained by both methods. Figure 7 presents the plot of these data. Although it reaches -50° at the end of LS1, the cavity-to-cavity difference is within 1°. A closer look at the phase scans revealed that the two-harmonic approximation returns about 0.5-deg-different points of maximum energy gain, which ALPha uses to set the operating phases. We assume this value is the accuracy of the existing IPS model.

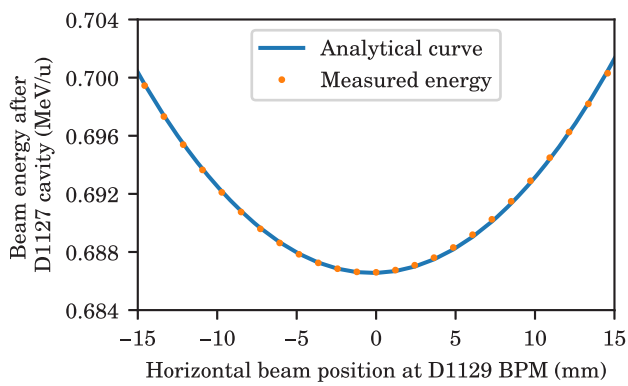

Figure 8: Transverse-longitudinal coupling in a cavity.

ISBN: 978-3-95450-232-5 ISSN: 2673-7000 doi:10.18429/JACoW-NAPAC2022-THZD1

We experimentally studied the transverse-longitudinal coupling in the beam acceleration and found it in perfect agreement with analytical estimates, see Fig. 8. We steered the beam upstream of the cavity and measured the output beam energy as well as the beam position at the nearest downstream BPM. From geometrical calculations, we found the beam position at the cavity center and put it into an argument of the modified Bessel function [6]. This coupling is an important factor for cavity calibration. It also contributes to the beam energy gain through the finite beam size even if the beam is aligned to the cavity axis.

Envelope Mapping

Another technique that we implemented to verify the IPS tunes is the longitudinal envelope mapping. It is an extension of the SNS "longitudinal shaking" method [26]. By detuning the phases of the MEBT bunchers, the beam center can be mismatched in the phase-energy domain in a way that it appears on the rms ellipse (estimated from simulations) at the LS1 entrance. The mismatched beam trajectory then represents the phase trajectory of a particle as if it originated at the mismatched beam center. This trajectory can be measured by the linac BPMs. If one evaluates other points on the same rms ellipse, the BPM phases show the transformation of the initial ellipse along the linac. The envelope of these trajectories becomes the rms envelope.

It is important to note that this is not a measurement of the rms bunch length, this is only a mapping of a given initial phase-space ellipse. Moreover, this method does not do correct mapping in the post-stripper part of the linac, because it cannot handle the longitudinal emittance growth due to energy straggling in the stripper. However, if the emittance growth is not very large, the envelope mapping gives a good understanding of the envelope matching and stability of the beam motion. An example of the envelope mapping in the whole FRIB linac is presented in Fig. 9.

Bunch Length Measurements

To make the envelope mapping data actually represent the beam envelope, we need to measure the bunch length in several points along the linac and match it to the mapped envelope. The measurements also give an estimate of real beam emittance. An easy and convenient way to measure the bunch length is the acceptance scan method [27, 28]. We shift the phases of LS2 cavities by the same angle and make the longitudinal acceptance shift relative to the beam. Then the derivative of the measured LS2 transmission curve becomes the longitudinal beam profile. We performed these measurements in several places in LS2 and got information about the bunch length variation (an indicator of the beam envelope mismatch) and the variation of bunch position relative to the reference particle (an indicator of the beam trajectory mismatch). The information about the bunch trajectory is particularly important for the multiple charge state acceleration in LS2 [29]. An example of the bunch length measurement in LS2 is shown in Fig. 9.

CONCLUSION

The presented IPS model has been implemented in a new HLA and is used routinely for the FRIB linac operations. Its superior capabilities have been demonstrated during the beam commissioning of a new FSEE beamline of the linac (see Fig. 1) [30], when during one evening we developed, applied, and tested four different velocity profiles in LS1 for three different ion species: $^{40}Ar^{14+}$ at 36.6 MeV/u, $^{16}O^{7+}$ at 41 and 44.7 MeV/u, and $^{129}Xe^{28+}$ at 27 and 15 MeV/u (these two share the same velocity profile). During one of the FSEE experiments a faulty cavity had been bypassed in only 10 minutes and the beam energy was recovered.

The IPS model was successfully applied to setup beams for the first three FRIB user experiments. For example, the settings for the first experiment were established by one accelerator physicist in 6 hours from the ion source to the beam dump at the end of LS3.

The IPS is planned to be applied for the phasing of the MSU ReAccelerator facility which currently relies on the time-consuming Si-detector energy measurements [8].

ACKNOWLEDGEMENTS

The authors thank Andrei Shishlo from the Accelerator Physics group of SNS for sharing their accelerator tuning experience. The authors thank Dan Morris and Shen Zhao from the FRIB RF and LLRF groups for discussions of RF circuits; Steve Lidia and Scott Cogan from the FRIB BIM department for discussions of BPM measurements.

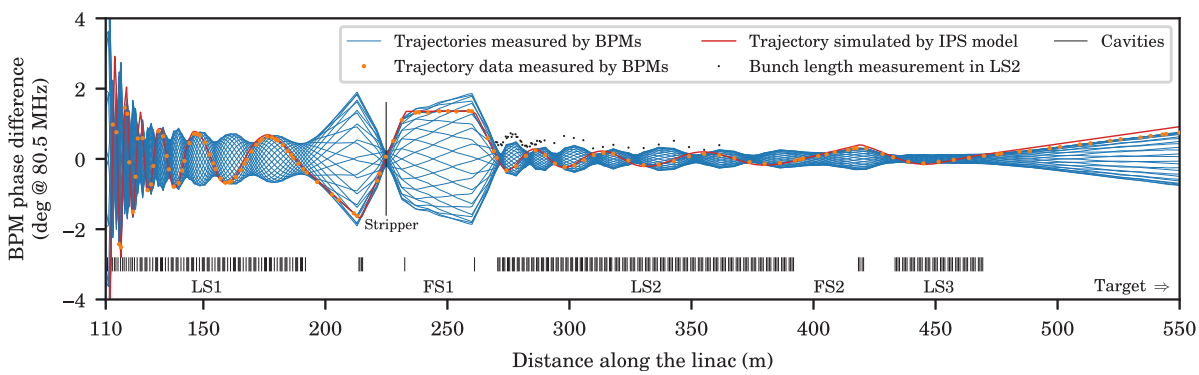

Figure 9: Envelope mapping result and rms bunch length measured in LS2.

ISBN: 978-3-95450-232-5 ISSN: 2673-7000 doi:10.18429/JACoW-NAPAC2022-THZD1

REFERENCES

[1] J. Wei *et al.*, "FRIB Commissioning and Early Operations", in *Proc. IPAC'22*, Bangkok, Thailand, Jun. 2022, pp. 802-807. doi:10.18429/JACoW-IPAC2022-TUIYGD3

[2] T. Xu *et al.*, "SRF Development and Cryomodule Production for the FRIB Linac", in *Proc. NAPAC'16*, Chicago, IL, USA, Oct. 2016, pp. 847–852. doi:10.18429/JACoW-NAPAC2016-WEB3IO01

[3] K. Saito *et al.*, "Superconducting RF Development for FRIB at MSU", in *Proc. LINAC'14*, Geneva, Switzerland, Aug.-Sep. 2014, paper THIOA02, pp. 790–794.

[4] C. Compton, "FRIB Cavities and Cryomodule Production", presented at LINAC'18, Beijing, China, Sep. 2018, paper TU1A04, unpublished.

[5] E. S. Lessner and P. N. Ostroumov, "Reliability and Availability Studies in the RIA Linac Driver", in *Proc. PAC'05*, Knoxville, TN, USA, May 2005, paper FOAC005, pp. 443–445.

[6] T. P. Wangler, *RF Linear Accelerators*, Weinheim, Germany: Wiley-VCH, 2008.

[7] A. C. C. Villari, D. B. Crisp, A. Lapierre, S. Nash, T. Summers, and Q. Zhao, "Energy Calibration of the Rea3 Accelerator by Time-of-Flight Technique", in *Proc. IPAC'19*, Melbourne, Australia, May 2019, pp. 2760-2762. doi:10.18429/JACoW-IPAC2019-WEPGW112

[8] D. J. Barofsky *et al.*, "Automation of the ReAccelerator Linac Phasing", in *Proc. IPAC'21*, Campinas, Brazil, May 2021, pp. 2170-2172. doi:10.18429/JACoW-IPAC2021-TUPAB292

[9] A. C. C. Villari *et al.*, "Reaccelerator Upgrade, Commissioning and First Experiments at The National Superconducting Cyclotron Laboratory (NSCL)/Facility For Rare Isotope Beams (FRIB)", in *Proc. IPAC'22*, Bangkok, Thailand, Jun. 2022, pp. 101–103. doi:10.18429/JACoW-IPAC2022-MOPOST021

[10] M. Ikegami, Y. Kondo, and A. Ueno, "RF Tuning Schemes for J-PARC DTL and SDTL", in *Proc. LINAC'04*, Lübeck, Germany, Aug. 2004, paper TUP65, pp. 414–416.

[11] S. Canella, "An Automatic Procedure to Find and Set the Shift Phases for the Superconducting Resonators in the ALPI Accelerator", in *Proc. of ICALEPS'97*, Beijing, China, Nov. 1997, p.113-115.

[12] A. P. Shishlo, "Model and Beam Based Setup Procedures for a High Power Hadron Superconducting Linac", in *Proc. LINAC'14*, Geneva, Switzerland, Aug.-Sep. 2014, paper MOIOC03, pp. 41–45.

[13] N. Milas, C. Plostinar, R. Miyamoto, M. Eshraqi, and Y. Liu, "Position-based cavity tuning", *Phys. Rev. Accel. Beams*, vol. 23, p. 114002, Nov. 2020. doi:10.1103/PhysRevAccelBeams.23.114002

[14] S. I. Sharamentov, R. C. Pardo, P. N. Ostroumov, B. E. Clifft, and G. P. Zinkann, "Superconducting resonator used as a beam phase detector", *Phys. Rev. ST Accel. Beams*, vol. 6, p.052802, May 2003. doi:10.1103/PhysRevSTAB.6.052802

[15] N. R. Lobanov, "Superconducting resonator used as a phase and energy detector for linac setup", *Phys. Rev. Accel. Beams*, vol. 19, p. 072801, Jul. 2016. doi:10.1103/PhysRevAccelBeams.19.072801

[16] W. K. H. Panofsky, "Linear Accelerator Beam Dynamics", University of California, Berkeley, CA, USA, Rep. UCRL-1216, Feb. 1951.

[17] J. R. Delayen, "Longitudinal transit time factors of short independently phased accelerating structures for low velocity ions", *Nucl. Instrum. Methods, A*, vol. 258, p.15-25, 1987. doi:10.1016/0168-9002(87)90076-3

[18] A. Klebaner *et al.*, "Overview of Progress in The Construction of the PIP-II Linac", in *Proc. SRF'21*, East Lansing, MI, USA, Jun. 2021. doi:10.18429/JACoW-SRF2021-MOOFAV05, to be published.

[19] G. Devanz, "SPIRAL 2 Resonators", in *Proc. SRF'05*, Ithaca, NY, USA, Jul. 2005, paper MOP02, pp. 108-112.

[20] The beam dynamics code TRACK, http://www.phy.anl.gov/atlas/TRACK

[21] S. Zhao *et al.*, "Automation of RF and Cryomodule operation at FRIB", presented at HIAT'22, Darmstadt, Germany, Jun. 2022, paper TH1C3.

[22] W. Chang *et al.*, "Automation of superconducting cavity and superconducting magnet operation for FRIB", presented at NAPAC'22, Albuquerque, New Mexico, USA, August 2022, paper MOPA83, this conference.

[23] A. P. Shishlo, "Benchmark of Superconducting Cavity Models at SNS Linac", in *Proc. IPAC'21*, Campinas, Brazil, May 2021, pp. 671–674. doi:10.18429/JACoW-IPAC2021-MOPAB203

[24] R. E. Shafer, "Beam position monitoring", *AIP Conference Proceedings*, vol. 249, p.601, 1992. doi:10.1063/1.41980

[25] CST Studio Suite, https://www.3ds.com/products-services/simulia/products/cst-studio-suite/.

[26] A. P. Shishlo and A. V. Aleksandrov, "Using the Online Single Particle Model for SNS Accelerator Tuning", in *Proc. HB'08*, Nashville, TN, USA, Aug. 2008, paper WGB06, pp. 203–206.

[27] A. Shishlo, A. Aleksandrov, Y. Liu, and Z. Wang, "Measuring longitudinal beam parameters in the low energy section of the Oak Ridge Spallation Neutron Source accelerator", *Phys. Rev. Accel. Beams*, vol. 21, p. 092803, Sep. 2018. doi:10.1103/PhysRevAccelBeams.21.092803

[28] A. Chao, K. Mess, M. Tinger, and F. Zimmerman, *Handbook of Accelerator Physics and Engineering, 2nd ed.*, Singapore: Scientific, 2013.

[29] P. N. Ostroumov, K. Fukushima, T. Maruta, A. S. Plastun, J. Wei, T. Zhang, and Q. Zhao, "First Simultaneous Acceleration of Multiple Charge States of Heavy Ion Beams in a Large-Scale Superconducting Linear Accelerator", *Phys. Rev. Lett.*, vol. 126, p. 114801, Mar. 2021. doi:10.1103/PhysRevLett.126.114801

[30] S. Lidia *et al.*, "A Heavy-Ion Single-Event Effects Test Facility at Michigan State University", in *Proc. 2022 IEEE Radiation Effects Data Workshop (REDW) (in conjunction with 2022 NSREC)*, Provo, Utah, USA, Jul. 2022, to be published.